JET–P(97)06

Prediction/Modelling of the Neutron Emission from Hot-ion H-mode Discharges

O N Jarvis.

JET Joint Undertaking, Abingdon, Oxfordshire, OX14 3EA, UK.

Preprint of a paper to be submitted for publication in
Plasma Physics and Controlled Fusion

March 1997

ABSTRACT

A simple 0-D computer code has been prepared for *predicting* the neutron emission in the initial phase of beam-heated hot-ion H-mode discharges in the Joint European Torus (JET). It performs very well for discharges with low particle recycling up to the onset of MHD-related activity, which usually occurs within one second of commencing full power heating. It can also be used to *model* the entire discharge, including the termination, when fuelling of the plasma core with cold neutrals is adopted as a first-order approximation for edge recycling effects. Specifically, given the time traces for the beam heating power, the global neutron emission, average electron density, Zeff and Dα signals, the code can satisfactorily reconstruct the core volume rotation rate, ion temperature and electron temperature for the entire duration of the discharge, and it also provides an explanation for the anomalously low burnup of d-d fusion product tritons that is sometimes observed. The code provides insight into the relative intensities of the three contributing reaction mechanisms to the total neutron emission (thermal, beam-thermal and beam-beam reactions) as an aid to interpretation of data from the various neutron diagnostics on JET, including the neutron profile monitor and the neutron spectrometers. Tritium fuelling and beam injection are also implemented, so the code can be used to extrapolate the neutron emission from existing d-d discharges to that expected from similar d-t discharges.

1. INTRODUCTION

A simple 0-D computer code has been prepared for predicting the neutron emission in the initial phase of beam-heated hot-ion H-mode discharges. The initial motivation for developing the code stemmed from the intuitive belief that, because the electron density radial profile is approximately flat for JET H-mode discharges, it should be possible to predict the initial rate of rise of the neutron emission with fair accuracy from first principles without requiring empirical ion and electron density and temperature profiles and that a near perfect fit should be obtainable by introducing just one or two empirical parameters. In practice, the calculation proved successful and the results were at most weakly dependent on the values chosen for these parameters. It was found subsequently that by approximating the density increase due to edge recycling by the addition of cold neutral particles to the plasma, then not only could the initial rise phase of the neutron emission be modelled for discharges with significant recycling, but the collapse phase could be modelled also. That the code should perform very well during the rise phase of good discharges is easily understandable on the basis of simple physical principles. That the trivial concept of fuelling through incursion of cold neutral particles should not only be useful for modelling the neutron emission from high recycling discharges but should also produce core plasma properties of rotation rate, ion and electron temperatures that correspond well with their experimental values is both surprising and suggestive. It is noted that a high neutral density

during giant ELMs provides a possible explanation for the observed anomalously low burnup of 1.0 MeV tritons produced from d-d fusion reactions.

2. OUTLINE OF THE MODEL

For clarity of presentation, we consider first the idealized model in which the plasma fuelling is solely attributable to beam particle injection. This is the zero recycling approximation in which there is no gas puffing and no wall pumping to be taken into account. These, and other, complications will be included in the modified model, to be described subsequently. The idealized model is suitable for predictive or scoping studies but the modified model is required when it is desired to simulate actual discharges as faithfully as possible.

2.1 The ideal model

The ion and electron density profiles are taken as being flat over the entire plasma, a fairly good approximation for H-mode discharges. The temperature profiles are taken to be stepped, with a core volume with average temperatures Ti_0 and Te_0 and a peripheral volume with ion and electron temperatures half the central electron temperature, to approximate the observed volume averaged temperatures. In the absence of experimental neutron emission profile data, the extent of the core volume is arbitrarily defined as being the volume occupied by the plasma current assuming a uniform current density with safety factor q = 1. As will be discussed in section 3.1, the neutron emission strength is relatively insensitive to the extent of the core volume. The neutron emission is broken down into the usual three components: the thermal, beam-plasma and beam-beam neutron production rates. The thermal neutron emission is restricted to the core volume. Since $Ti_0 \sim 2\ Te_0$ and the thermal fusion reactivity scales roughly as Ti^2 for high Ti and more strongly for low temperatures, the thermal contribution from the peripheral volume is expected to be relatively small for the cases of current interest, even though the core to peripheral volume ratio is typically 1:6. The beam-plasma neutron production is approximately equally divided between core and periphery for the highest performance discharges. Beam-beam neutron production is a strongly peaked central feature when the beams are well focused since it depends on the square of the fast ion density. Normally, the beam-beam contribution is very small but it has to be calculated in case circumstances cause it to become important. A full calculation requires a Monte Carlo approach such as that implemented in the code TRANSP [1]; accordingly, the model employs a simple calculation based on the fast ions being averaged over the core volume but makes reference to TRANSP calculations to obtain a suitable scaling factor, interpreted by defining an innermost volume that contains the desired fast ion population. This scaling factor need be determined only once for a given beam-line geometry. Thus, the model contains three volume elements.

The geometry of the plasma is such that the volume elements are elliptical and possess a common centre. The peripheral volume and its elongation are given values appropriate to the discharge under study. The core volume and elongation are determined by comparison with the profiles measured with the JET neutron profile monitor [2,3]. The innermost region takes the same elongation as the core but has a volume derived from TRANSP, as mentioned above. The geometrical arrangement of the plasma volumes and the lines-of-sight of the profile monitor are shown in fig.1 for discharge 25432, which was run in a single null X-point configuration, the Mk.0 divertor, with the plasma axis situated near the median plane of the vacuum vessel. The beam injection geometry is simplified by assuming the beam-lines to lie in the horizontal median plane of the tokamak but the injection angles of the normal and tangential beams are otherwise respected. This geometry results in the beam lines all crossing the axis of the plasma column. Such an arrangement is unrealistic but is nevertheless an adequate representation for the present circumstances where the core volume is relatively large (the core diameter being more than one third the plasma column diameter). For later discharges run after the pumped divertor was installed, the Mks. I and II configurations, the plasma axis was raised by about 0.3 m so as to provide clearance above the in-vessel divertor coils. At the same time, the beam lines were adjusted in an attempt to refocus on the plasma axis but full compensation for the changed geometry was not possible and the beams were spread vertically to a greater extent than before and the beam deposition profile, and resulting temperature profile, were both less strongly peaked; these broader profiles are favourable for the present model.

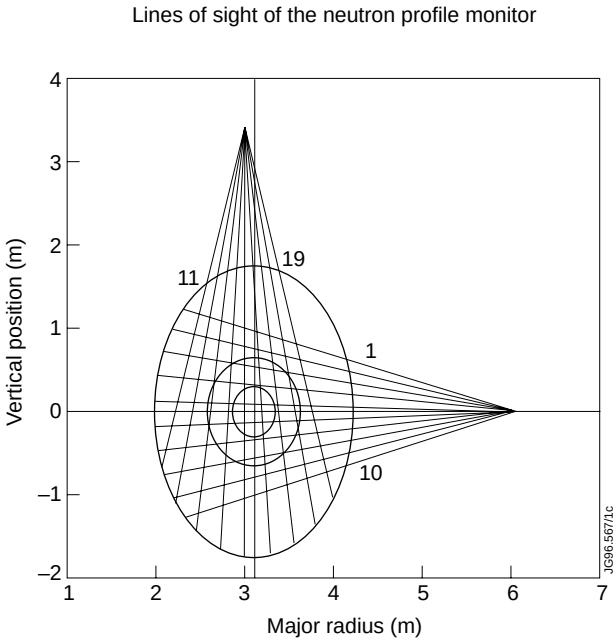

Fig.1: Illustrating the plasma geometry adopted for the model, together with the 19 lines-of-sight (channels) from the neutron profile monitor. The channels are numbered 1 through 10 for the horizontal viewing camera (which gives a vertical profile) and from 11 to 19 for the vertical viewing camera (which gives a horizontal profile).

For the ideal model, only the initial plasma conditions of electron density, Zeff (one major impurity component), central ion and electron temperatures are required, along with the plasma external dimensions and the plasma current and toroidal field strength. The neutral beam heating powers, energies and molecular fractions are all taken into account. Tritium beam injection is also modelled, but will not be discussed further. The beam particle deposition in the core volume is computed and fast ion energy is shared between the background ions and electrons through a multi-group time-dependent slowing down calculation. Plasma rotation is implemented through a classical calculation of momentum transfer from the beam ions to the plasma core. A further

assumption is that the beam ions thermalize within their deposition volumes and only thermal particles diffuse out across the core boundary so as to maintain a completely flat density profile. In this way a convective term is introduced implicitly.

An arbitrary energy sink term is needed to represent ion and electron energy conduction losses. Accordingly, the ITERH93-P scaling law [4] was adopted as the means for determining the overall energy loss rate from the plasma, permitting the study of H-mode discharges in machines of widely differing sizes. A multiplicative factor is employed so that enhanced or degraded confinement can be simulated; however, the relative loss rates from ion and electron channels remain to be determined empirically. It was quickly discovered that ion conduction losses can usually be neglected. Similarly, there appears to be no need to model charge-exchange losses involving the cold electrons deposited by the ionizing beam neutrals; presumably, re-ionization is rapid and there must be an approximate cancellation across the core boundary of incoming and outgoing secondary neutral particles.

An example of the performance of the ideal model in a purely predictive mode is shown in fig. 2 for discharge 33643. This discharge produced one of the highest instantaneous neutron emission strengths for JET d-d discharges but is otherwise typical of all good quality hot-ion H-mode discharges, which implies minimal gas fuelling through recycling at the walls. It terminated abruptly due to a simultaneous sawtooth crash and a giant ELM, neither of which are simulated. Another complication that is not simulated is the rapid fall in density during X-point formation before the application of beam heating; instead, it is assumed that the dump plates became saturated so that pumping ceased before the beams were switched on. The only time-dependent data input to the code are the beam powers. The initial electron density, ion and electron temperatures, and Zeff values are taken to be those just before beam switch-on. The core volume is derived from comparison of predicted and measured neutron emission profiles but, as will be explained below, the predicted neutron intensity is insensitive to the precise value chosen. Two computed time-traces are shown. The first (the dotted curve), which assumes perfect thermal confinement in the core, fits the rising slope of the measured neutron emission almost

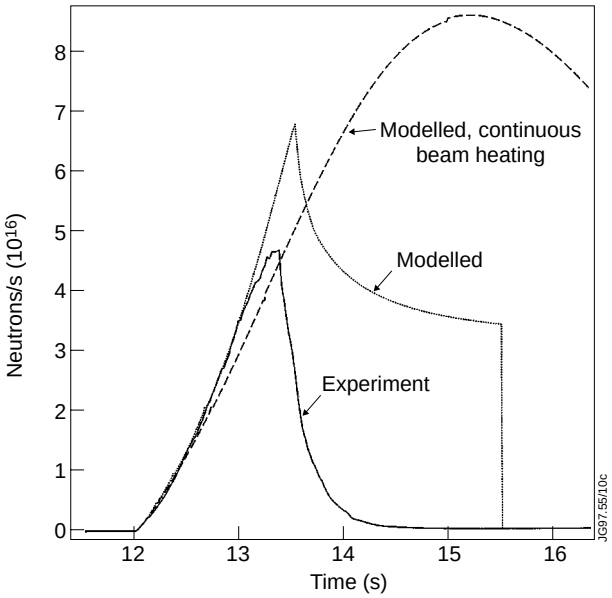

Fig.2: Comparing the measured time-resolved neutron yield for d-d discharge 33643 with two predictions of the ideal model. The dotted curve assumes perfect thermal confinement and beam heating that terminates just after the collapse of the measured neutron emission. The dashed curve predicts the performance when the beam heating is continued indefinitely and the conduction losses are set at a value typical for discharges that survive more than 1 sec.

perfectly. The beam heating terminates just after the collapse of the actual discharge and the fall in predicted emission is due to equilibration between ions and electrons. The second time-trace is an attempt to estimate to what height the neutron yield might have risen had the beam heating continued indefinitely, in the absence of MHD phenomena. For this case, the ITERH93-P scaling law was used to determine the power loss rate from the core plasma, with a multiplying factor of 0.25, corresponding to an H-mode enhancement factor H_{93} for the whole plasma of about 2, and with losses restricted to the electron channel only. Experience has shown this to be typical of H-mode discharges that survive with good confinement long enough for the loss rate to become comparable with the input power. It is seen that the fit to the experimental neutron intensity is remarkably good for the first 0.5 s, thereafter falling below the measured intensity but eventually reaching saturation at double the observed maximum as a result of the electron density increasing due to beam fuelling until the energy loss rate exceeds the power input.

If desired, the effects of wall pumping, gas fuelling and changes in discharge quality due to sawteeth or changes from L to H-mode confinement can be studied separately or together. An exponential decay of the particle density is achieved through a particle confinement time that affects all particles equally. Gas fuelling is implemented by introducing cold deuterium atoms at a rate proportional to the beam power, the proportionality constant sometimes being called the fuelling ratio. The neutrals are deposited uniformly throughout the plasma, this being the only practical means of approximating diffusion processes. When examining real discharges, it is obviously difficult to separate clearly the effects of pumping from gas fuelling but a good approximation is that pumping ceases while the plasma is in the H-mode regime. Sawteeth are modelled pragmatically, by abruptly reducing the core temperature in line with experimental observations. Confinement quality is represented by converting the energy loss rate multiplying factor into a programmable time trace. The change from L to H-mode confinement has to be incorporated in discharges with extended periods of low power beam pre-heating prior to application of full power (as in discharge 26087, to be examined later). In particular, the consequences of a giant ELM can also be represented by a sudden drop in confinement time to near zero for a few tens of milliseconds before restoring it to near its original value; this technique reproduces the behaviour of the ion temperature and neutron emission but does not correctly reproduce the electron temperature and does not affect the plasma rotation rate. Such abrupt changes [5] in plasma confinement time are unrealistic. The difficulties mentioned in this paragraph are circumvented when the measured electron density and Zeff time-traces are used as data input and gas fuelling is modelled as an influx of cold, non-rotating, neutrals using the $D\alpha$ signal as measure of the resulting neutral density and the artificial temporal separation of wall pumping from gas fuelling is removed (section 2.2).

A neutron signal of considerable interest is the 14 MeV neutron flux from t-d fusion reactions, where the 1.0 MeV tritons from d-d fusion reactions slow down in the background plasma and undergo fusion reactions with thermal deuterons. In the present model, the calculation

neglects the effects of real temperature profiles, of the finite banana widths of the triton orbits, and of the burnup of tritons with fast deuterons. Nevertheless, the model proves capable of simulating the actual triton burnup signal remarkably well for discharges that have graceful terminations. For hot-ion H-mode discharges, the terminations usually occur abruptly near peak performance due to giant ELMs and carbon blooms. In such cases, the termination of the discharge has to be modelled faithfully if any useful conclusions are to be drawn concerning the magnitude of the burnup signal. It is for this reason that the d-d neutron yields for the discharges discussed in this paper were modelled with particular care.

2.2 The modified model

Unfortunately, there are relatively few discharges for which the plasma boundary recycling can be ignored. Gas puffing is used both for fuelling and to inhibit early MHD phenomena, whilst strong wall pumping is experienced as the plasma enters the X-point configuration or whenever the plasma is pushed against a boundary surface to terminate a discharge without provoking a disruption. Gas fuelling and edge recycling are simulated by an assumed influx of neutrals proportional to the intensity of the $D\alpha$ light emitted from the plasma boundary. That neutrals can travel significant distances into a plasma (perhaps tens of centimetres in the present situation) is a consequence of the high edge temperatures (~ 3 - 5 keV) and the very narrow boundary zone (width ~ 1 cm). The likely consequences of strong influxes of neutral particles have recently been considered by Christiansen and Muir [6]. That incoming neutrals should uniformly populate the core volume, as assumed here, is a convenient fiction. The actual arrival of cold neutrals in the core would have multiple consequences: they would (i) act as a brake on the plasma rotation, (ii) fuel the plasma, (iii) dilute the impurity content, (iv) effectively cool both ions and electrons. These effects are included in the modified model. L-H mode and reverse transitions are represented through their characteristic steps in $D\alpha$ light intensity. A high neutral density in the peripheral volume provides a possible explanation for the lower than expected 14 MeV neutron production rate from burnup of d-d fusion product tritons through the escape from the plasma of neutralized tritons. Neutrals in the core, even if genuine and not just a convenient mathematical device, would not lead to detectable triton losses because the path length before re-ionization is relatively short. Given this means for cooling the plasma, the ion and electron conduction loss terms are now set to zero for all but the power step-down discharges [7].

The modelling of an actual discharge demands that the experimentally determined electron density and Zeff data be reproduced. A typical set of time traces used as input to the code is presented in fig. 3. Occasionally, the central density is appreciably greater than the volume averaged density. In this situation, the axial density is adopted and the plasma outer volume is reduced so as to conserve particle numbers. The model is not readily capable of simulating discharges in which the Zeff is high and has a strongly shaped profile. For such cases the effective Zeff can be derived from the initial rate of rise of the neutron emission rate at beam switch-on,

which is sensitive to the n_d/n_e density ratio. Preferably, the analyses are restricted to low Zeff discharges (Zeff < 2) where this problem is minimized.

There are several Dα signals available that can be used to indicate the strength of the neutral influx, but they are local rather than global in nature and so, while they all display the same time sequence of major events (ELMs), their amplitudes may differ and, sometimes, features present in one are absent from another. Thus, the adopted Dα signal should be regarded as providing merely a rough template for the evolution of the neutral influx.

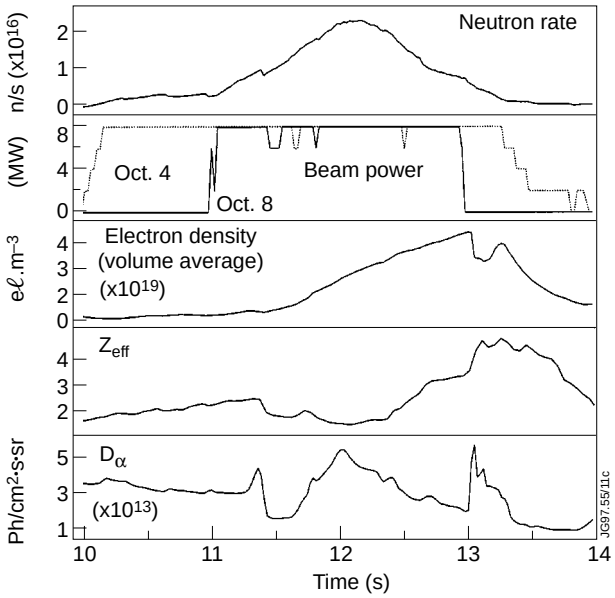

Fig.3: Showing the neutron yield for discharge 25432, along with the time-traces required as input for the modified model. These are the beam powers (two traces, corresponding to the two beam injectors), the volume-averaged electron density, the Zeff signal (usually derived from charge-exchange measurements) and the Dα signal.

The influx of cold neutrals is first of all set at such a level that the measured electron density is reproduced. If there is any over-fuelling, the code will automatically lower the density so as to recover the target (i.e. measured) density by removing (pumping out) thermal ions and electrons. This over-fuelling is frequently demanded by the need to dilute the impurity concentration down to the measured concentration. In addition to these constraints, the influx of non-rotating neutral particles may have to be enhanced even further to brake the rotation of the plasma in accordance with observations. These requirements are satisfied prior to carrying out the heating calculation, by initially setting the overall normalization factor for the Dα signal (i.e. the neutral density) and iterating as necessary. The heating and neutron production calculations can then be carried out. It is frequently found that an acceptable envelope for the neutron emission is immediately obtained; if not, it can improved by making further iterative adjustments of the normalization factor. For demonstration purposes, the temporal behaviour of the neutral density can be adjusted so as to provide as close a fit to the total neutron emission as desired. The core ion and electron temperatures are then found to agree rather well with their measured counterparts. Finally, the triton burnup calculation is performed.

It is found empirically that the Dα signal normalization factor does not change greatly with discharge type and corresponds to about 1 neutral introduced into the plasma per Dα photon. This influx is an order of magnitude greater than the result 1 neutral for every 10 to 20 Dα photons as calculated from the basic atomic cross-sections [8] for typical edge plasma conditions.

2.3 Data quality and consistency

The highly approximate nature of any 0-D computer model will obviously be uppermost in mind when comparing its predictions with measured plasma parameters. However, it should not be forgotten that the parameters determined experimentally are themselves subject to substantial experimental uncertainties. Thus, forcing agreement with particular parameters can be a major mistake. A certain amount of intuitive editing is frequently necessary and is, indeed, a normal feature of performing TRANSP analyses.

3. SOME PHYSICS CONSIDERATIONS

At first sight, it would not be expected that the ideal model could predict the neutron emission during the rise phase with any accuracy without optimization of adjustable parameters. In practice, it does so and there are good reasons for this performance, as will be explained in the following sections. That the modified model can then be used to reproduce the neutron emission during an accelerated termination, while also approximately reproducing the electron temperature and rotation rate, is less obvious.

3.1 Volume of the core region

Without prior information, the core volume used in the code is specified in terms of the plasma current density. However, at JET, the neutron emission profiles are routinely measured and can be used to define a precise core volume; examples will be provided later, for each of the two main divertor geometries. Interestingly, the total neutron emission from the plasma is remarkably insensitive to the volume assumed for the core, varying by only 20% when the core volume is increased from one quarter up to the whole plasma volume. This can be understood in the approximation that the fraction of beam particles deposited in the core volume scales linearly with the diameter of the core. The number of ions and electrons onto which the beam energy is deposited scales quadratically with the diameter and the temperature of the ions will scale inversely to their number. For hot-ion discharges, the thermal neutron emission scales quadratically with the product of deuterium density and temperature. The net result is that the thermal neutron emission is unaffected by a change in core volume. When the core volume is reduced and beam penetration is taken into account, the computed temperature and therefore the beam-plasma neutron emission are found to increase but the thermal emission falls and the total neutron emission is little changed. Of course, the use of the correct core volume does become important with regard obtaining realistic temperatures, needed for determining the precise ratio of thermal to beam-plasma neutron emission and for predicting the triton burnup.

The volume and elongation of the boundary surface for the peripheral volume are taken from the magnetic reconstructions. The core volume is determined from comparison of the initial model predictions for the line-integrated fluxes along the lines-of-sight of the JET neutron profile

monitor with the experimental data. Despite the simplicity of the model, the comparison permits the volume and elongation of the core to be estimated rather precisely. The neutron profiles used are those for times close to that of peak neutron emission, since the plasma conditions at peak performance are of greatest interest. It is implicitly assumed that the core geometry is fixed throughout the discharge. Fortunately, it so happens that the experimentally determined profile shapes do not change appreciably during the entire beam-heating period. Sawteeth produce only transient effects.

3.2 The neutron emission immediately following beam switch-on

At the moment of abrupt switch-on of the neutral beam injection, and for tens of milliseconds thereafter before the more energetic of the injected fast ions have time to slow down appreciably, the gradient of the neutron emission curve against time depends mainly on the beam-plasma neutron production rate and is a sensitive measure of the volume-averaged n_d/n_e ratio, or Zeff, assuming that n_e and the major impurity are known. The calculation does require the initial plasma conditions to be defined with some care as the beam shine-through must be computed. If the calculation fails to fit the initial slope of the neutron emission, then the most probable cause is an incorrect experimental determination of the n_d/n_e ratio.

3.3 Plasma rotation

Because of the inclined beam injection angles, JET hot ion discharges can achieve high rotation rates. Naturally, there is considerable shear in the rotation rate but for the present model the core is considered to rotate as a rigid body with no interaction with the surrounding peripheral plasma. The rotation rate can be calculated from simple considerations of momentum transfer. It is unnecessary to introduce a finite momentum time constant in the modified model because the incursion of non-rotating cold neutrals provides the required braking action. To model the measured rotation, it is appropriate (for high performance discharges) to assume that the fast ions deposit their momentum instantly on the background thermal particles. The justification for this is that the ion-ion collision time for the high energy component of the injected ions is up to an order of magnitude shorter than their slowing down time in hot plasmas so that pitch-angle scattering suffered by passing beam ions will rapidly lead to their becoming trapped, with the momentum transfer taking place in the collisions that cause the trapping. Subsequent detrapping will result in almost equal numbers of co- and counter-passing particles and will have no net effect on plasma rotation.

It is a general finding that the measured rotation rates in Mks. I ands II divertor geometries reach peak values more than 40% greater than those recorded prior to the installation of the pumped divertor. Investigations with the code show that the simplistic differences involving plasma volumes, beam energies, beam focussing, plasma densities, etc. do not explain the higher rotation rates. Instead, the most probable cause is the differing levels of edge recycling in the

different campaigns. Specifically, heavy gas puffing was frequently employed before the divertor was installed (e.g. for 25432 and 26087), whereas afterwards the gas puffing was much reduced (absent at beam switch-on for 33643, 34236 and 34500).

3.4 Beam-plasma reaction rates

Passing particles moving in the direction of rotation appear to the plasma to have reduced energy, and therefore reduced reactivity. Trapped ions are alternately viewed by the plasma as having lower and then enhanced energy, with the averaged reactivity being close to the reactivity of the injection energy [9]. The same argument that leads to momentum being transferred promptly also implies that it is a good approximation to regard all injected beam ions as being effectively trapped, since merely having been trapped briefly is sufficient to provide equal numbers of co- and counter-passing particles. Thus, when the effect of pitch-angle scattering is included for consistency with the calculation of plasma rotation, the beam-plasma emission is found to be very close to the TRANSP level; if trapping effects are neglected, the beam-plasma emission falls by 30 - 40%. That the highest energy group of the fast deuterons should suffer appreciable pitch-angle scattering while still at their peak nuclear reactivity is unexpected and is a feature specific to hot-ion discharges. The measured neutron energy spectra [10] for such discharges do have a strongly Gaussian appearance, compatible with a nearly isotropic fast ion distribution.

The local steady-state beam-plasma neutron emission per beam ion is given by

$$Y_{bp} = \left(\frac{n_d}{n_e} \right) n_e \int \langle \sigma v \rangle dt$$

Note $\int \langle \sigma v \rangle dt$ scales as $1/n_e$ and does not depend on Zeff. Thus, Y_{bp} is almost independent of n_e , varying with Zeff , however, and for high temperature plasmas Ti (~ 2×Te ~ 20 keV) scales approximately with the product $E_{beam}^{2.5}\, Te^{0.3}\, Ti^{0.6}$ for 100 keV beam ions.

The peripheral temperatures required to reproduce the observed volume averaged values are ~ 30% and ~ 60% of the core values, for ions and electrons, respectively; i.e. the peripheral ion and electron temperatures are approximately equal at about 6 keV for the best discharges. For these conditions Y_{bp} scales with temperature approximately as $Te^{0.4}\, Ti^{0.4}$ and the steady-state beam-plasma reaction rate per beam ion in the plasma periphery is approximately one half of that in the core (which value is used in the code). For the smallest core volume encountered in this work, the beam-plasma contributions from core and periphery are about equal, but the uncertainty in the global beam-plasma neutron emission introduced through this relatively crude assessment of the neutron emission from the periphery is unlikely to exceed 15%. This unexpected precision is partially attributable to the self-correcting nature of the calculation in which the computed total neutron emission is fitted to the experimentally determined emission (e.g. under-estimating the beam-plasma emission requires the ion temperature to be increased to obtain a fit to the total, and this results in the beam-plasma emission being increased).

3.5 Energy conservation

It is instructive to estimate the total neutron emission during the early heating stages for a highly idealized situation, comprising a single volume plasma possessing flat density and temperature profiles for which there is neither beam shine-through nor energy losses. Ion-electron energy equilibration is recognized by taking $T_i = 2\ T_e$. Given perfect energy confinement, the beam energy deposited, W, over time t since switch-on is used to heat cold ions and electrons to T_i, T_e, respectively. Clearly, for Zeff = 1 and low initial temperatures, $W = Pt = (9/4)\ n_d\ T_i$. With constant beam power, P, the density will rise linearly,

$$n_d = n_0 + (dn/dt)\ t, \text{ with } (dn/dt) \sim P/E\ V.$$

The thermal neutron emission scales as $n_d^2 T^{\alpha}\ V$, where V is the plasma volume and α is a temperature dependent parameter, being about 2 above 15 keV. For high temperatures, where the thermal emission is dominant, the total neutron emission will scale as W^2/V. Alternatively, after a given heating interval the thermal neutron emission rate will scale as $P^2\ t^2/V$. Note the inverse dependence on plasma volume.

The beam-plasma emission scales as the product of the number of injected ions of energy E and their fusion probability, or approximately as P T where we have neglected the dependence on E and use $T = T_i = 2\ T_e$. This can be expressed as $P^2\ t / n_d$, or $P^2\ t / (n_0 + P\ t / V)$. Thus, the beam-plasma emission rises linearly with time at first with a rate independent of volume and scaling with P^2, but eventually saturates at a level proportional P as the temperature rises asymptotically to the beam energy limit.

That the total neutron emission rate predicted by the code reproduces the measured rate rather faithfully during most of the emission rise phase is now understood to be a result of the energy loss rate from the plasma during this initial period being sufficiently weaker than the heating rate that it may be neglected for most good quality discharges. Thus, after 1 second, the typical duration of the high confinement phase of a hot ion discharge after which thermal reaction rate dominates over beam-plasma reaction rate, the neutron emission is nearly proportional to P^2. It has already been shown that the core volume is not a sensitive determinant of neutron emission.

3.6 Influx of cold neutrals

The concept that the core is fuelled exclusively by neutral beam deposition supplemented by an influx of cold neutrals from the edge, with no inwards diffusion of cold particles, may be little more than a mathematical simplification. However, diffusion is an inherently slow process, requiring several hundreds of milliseconds for cold ions to reach the plasma centre. Neutral particle cascades are effectively instantaneous. Thus, for modelling short-lived phenomena such as giant ELMs, the influx of cold neutrals does present itself as an obvious candidate, although

a measure of internal mixing due to a giant sawtooth crash or some other MHD effect appears to be an essential additional ingredient. For slower gas fuelling processes in relatively long-lived discharges, particle diffusion is the more relevant phenomenon but, even here, we might imagine that an influx of cold neutrals would provide a good first estimate of the effects of diffusion.

We next consider the problem of modelling edge recycling, with the effects of wall pumping and gas fuelling being inseparable. As already explained, the experimental volume-averaged electron density and Zeff data are regarded as a target values to be attained by adjusting the overall level of the neutral influx and the pumping strength to the necessary levels, with the core plasma rotation rate providing a further constraint. The numbers of fuel ions and electrons that are introduced into the core are determined by the fact that they are assumed cold and non-rotating. They could equally well be assumed to be warm and to possess the rotation of the edge region. Presumably, the net result with regard to rotation damping, density increase and impurity dilution would be much the same. The core ion temperature will attain the same value in both cases, as it is determined by the total neutron emission, but the electron temperature could be quite different. Also, the deduced pumping rates would probably differ.

3.7 The triton burnup measurements

Once the total d-d neutron emission has been modelled satisfactorily, the birth rate of fusion product tritons is also known, since the two branches of the d-d fusion reaction are approximately equally probable. Tritons are assumed to be fully confined and to slow down classically. As they slow down, their fusion reactivity increases until it reaches a maximum at about 200 keV, after which it declines sharply. The time dependence of the burnup signal depends mainly on the effective electron temperature, while the integrated burnup signal varies approximately as the product $(n_d/ne)T_e$. Since the burnup signal is delayed about 0.5 to 1 second after the d-d neutron signal, it affords an excellent probe of the decay phase of the discharge. In particular, it often reaches its maximum during the termination of the highest performance discharges and is therefore potentially a rich source of information.

Careful studies [11] have shown the burnup signal is very little affected by sawteeth. In fact, no change in the global emission is expected because the sawtooth crash merely redistributes the tritons within the plasma; their numbers and energies are unaffected and, to the extent that the plasma density and Zeff profiles are flat, then the instantaneous burnup rate will not alter. However, some discharges appear to exhibit anomalous losses of tritons [12], often considered to be diffusive losses even though the evidence strongly suggests that diffusion is entirely negligible [13,14]. It is proposed here that the anomalous losses are due to charge exchange events within the plasma periphery that lead to losses of neutralized tritons from the plasma.

3.8 The slow roll-over (X-event)

The slow-rollover, or X-event, is the name given to the slight, but sudden, change in slope of the increasing neutron rate, which usually just precedes a full saturation or even collapse [15]. It has not proven possible to explain this event solely as internal turbulence. For the Mk. 0 and the later Mk. I divertor geometries it is usually possible to relate the roll-over to an increase of the Dα activity prior to a giant ELM; as modelled in the code, the influx of cold neutrals proportional to the Dα signal is frequently found to reproduce the roll-over event. For the Mk II divertor geometry, the roll-over sometimes proceeds with no corresponding rise in the Dα signal. Instead, and contrary to previous experience, an increase in Zeff can sometimes be discerned at, or just prior to, the roll-over. Here we recognize that a change in the line-averaged Zeff signal must denote impurities entering from the edge and that diffusion to the core will be relatively slow, producing a delayed effect on the neutron emission. Thus, for the discharges modelled so far, the roll-over appears to be related to an influx of cold particles (either fuel or impurity ions) and is an inevitable response to a change in edge conditions.

3.9 Sawteeth

Sawtooth crashes are a distinctive feature of hot-ion discharges. However, only the final giant sawtooth crash that occurs at the collapse appears to have a lasting effect on the discharge. Largely for the sake of appearances, the sawteeth are modelled empirically by abruptly reducing the ion and electron temperatures in line with experimental observations.

4. SOME KEY FEATURES OF THE CODE

The code is designated NEPAM - Neutron Emission Prediction and Modelling. It is written in Mathcad 6+, a very high level language. The complete code requires a 100 MHz Pentium PC or faster, with at least 32 Mbytes of core storage. The running time of the code, using 10 ms time-bins and all options active, is about 20 minutes to simulate a 7 second discharge. Several iterations may be needed if faithful modelling of the collapse of a high performance discharge is required.

Most of the formulae used in the computer code can be obtained from “Tokamaks” by J.Wesson [16], but have to be modified for Zeff ≠ 1. The exceptions are the charged particle slowing down formula, for which the prescription of Stix [17] is adopted, and the beam-plasma and beam-beam fusion reactivities, which are computed using the relationships provided by Core and Zastrow [18].

5. EXAMPLES OF THE USE OF THE CODE

Five discharges have been selected to illustrate the performance capability of the code for d-d discharges. They include three of the best quality hot-ion H-mode discharges and two poor

quality discharges. The sequence of presentation is historical, and commences with a discharge for which the plasma conditions were far from those assumed by the model; indeed, it was selected because its poor performance was difficult to understand. The plasma volumes and elongations are presented for these five discharges in Table I, along with the electron density profile peaking factor (axial divided by volume-averaged density, further averaged over time), the beam powers, peak neutron emission rates achieved and the fuelling ratios. This last quantity is the ratio of fuelling through neutral influx (gas fuelling and recycling) to that by the beams, summed over the beam heating interval.

Table 1: Some characteristics of the selected discharges

Discharge number	**Volumes core & plasma (m^3)**	**Elongation core & plasma**	**Density peaking factor**	**Beam power 80keV & 140keV (MW)**	**Peak neutron yield (n/s)**	**Fuelling ratio**
25432	8.8 – 118	1.35 – 1.65	1.30	0.0 – 15.6	2.3×10^{16}	12.2
26087	15.2 – 114	1.35 – 1.70	1.50	4.0 – 10.9	4.3×10^{16}	4.2
33643	11.2 – 83	1.40 – 1.80	1.05	11.8 – 7.5	4.8×10^{16}	1.3
34236	17.6 – 78	1.45 – 1.70	1.10	11.0 – 7.4	3.1×10^{16}	0.9
34500	14.8 – 88	1.44 – 1.92	1.10	11.0 – 5.9	2.3×10^{16}	4.5

5.1 Discharge # 25432

Discharge No. 25432 was run in the tokamak as prepared for the JET PTE experiment [19], although in this case the X-point was formed on the lower, beryllium, dump plates. The plasma axis was 4 cm below the median plane of the machine and the beams were well focused at the centre. This naturally tended to produce a strongly peaked ion temperature profile, with moderate peaking of the density profile. The 140 keV beams were used, with a 1-second period of low power pre-heating to build up the ion density before the full 15.6 MW of heating power was applied (fig.3). The discharge was expected to display high performance (high neutron yields) but was marred by heavy gas puffing, intended to stabilize the discharge against early MHD effects. In practice, the gas puffing appears to have quenched the discharge through a strong inwards diffusion of cold fuel ions from the edge, which caused the ion temperature to be even more sharply peaked than it would otherwise have been, although the axial ion temperature did manage to rise to 18 keV before the diffusing cold ions reached the axis.

The neutron emission profile was so strongly peaked at the moment of strongest neutron emission that it proved impossible to simulate with only thermal and beam-plasma reactions. This is the only discharge so far studied that has demanded the inclusion of beam-beam reactions

in order that the neutron emission profile can be fitted. The difference between this discharge and others is that the thermal emission was not given a chance to grow, so that the peak emission corresponds to a time in the discharge when the beam-beam contribution was relatively large, although not unusually large in absolute terms.

The modelled and experimental neutron emission profiles corresponding to the moment of highest intensity are compared in fig. 4; the core volume and elongation have been adjusted to produce a good overall fit. The model reproduces the main features of the measured profile very well, considering the "top hat" nature of the temperature profiles adopted by the code. The experimental profile (denoted by the filled circles) is slightly narrower than the TRANSP prediction (crosses). Although the volume of the plasma was ~ 110 m^3, that of its core was only 8.8 m^3. As mentioned earlier, TRANSP calculations have been used to define the innermost volume used within the code for the beam-beam reactions (1.8 m^3 for 25432).

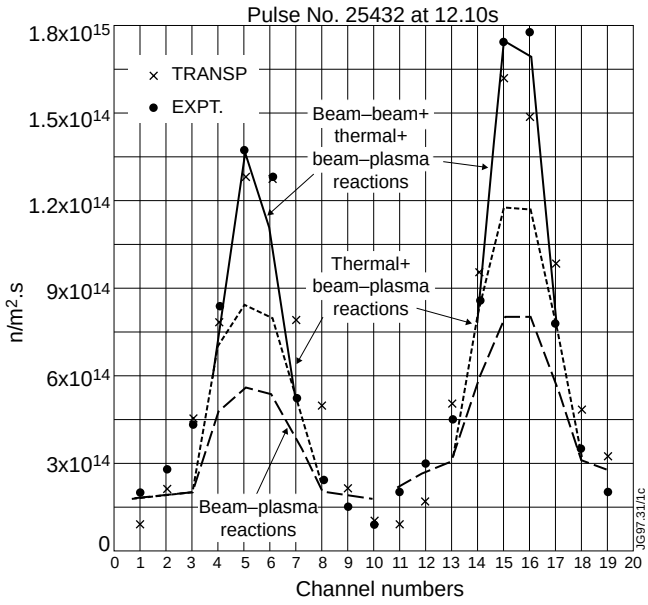

Fig.4: Comparing the predicted neutron emission profiles (lines) from thermal, beam-plasma and beam-beam reactions with experimental data (filled circles) recorded near peak performance for discharge 25432. The results of TRANSP simulations are also shown as crosses.

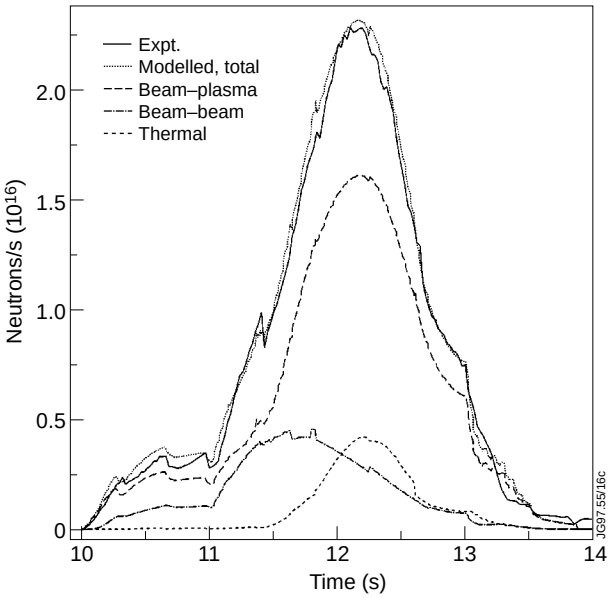

Fig.5: Showing the predicted neutron yields for the three neutron components for discharge 25432 . The dotted line represents the experimental total neutron yield. The results from the TRANSP simulation are similar. Note the very low thermal contribution.

The fit achieved to the time evolution of the total neutron emission is shown in fig. 5, together with the thermal, beam-plasma and beam-beam components. The beam-plasma contribution is large, about 70% of the total at the peak neutron emission rate; naturally, this is not a feature of a good quality hot-ion H-mode discharge. The beam-beam emission attains a strength slightly greater than the thermal component, but not at the same time. The corresponding results obtained using TRANSP are not shown separately since they are so closely similar;

however, the beam-plasma and beam-beam neutron emissions will be discussed in section 6, where the signals for all 5 discharges will be presented together.

The predicted 14 MeV neutron emission from triton burnup fits the measured signal approximately. This topic will discussed further in section 7.

In fig.6a the core rotation rate computed using the instant momentum transfer approximation is compared with the value derived from core-volume-averaged charge exchange recombination spectroscopy (CXRS) measurements [20]; these measurements are only available when the heating beam used as a source of charge-exchange neutrals is switched on. Fig.6a displays shows good agreement between code predictions and the measured CXRS rotation rate at peak neutron emission; this is expected, since the neutral influx has been adjusted iteratively until approximate agreement was indeed achieved and only minor adjustments were made subsequently.

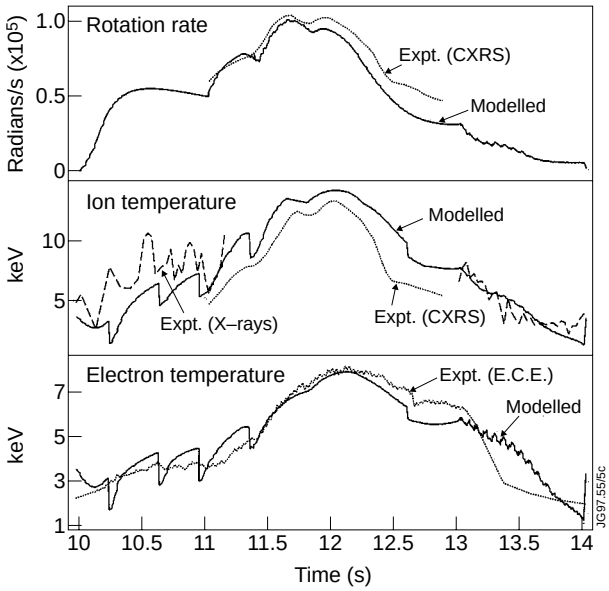

Fig.6: Comparing the predicted core rotation rate, ion and electron temperatures with core volume averaged experimental data for discharge 25432. The charge-exchange data are only obtainable during beam heating whereas the X-ray crystal data were only available when there was no beam heating.

Fig.6b compares the predicted ion temperature with the core *line-averaged* CXRS values. The temperatures measured using the X-ray crystal spectrometer [21] are also shown; this signal provides a local measurement at a point that varies in time as the plasma properties vary, approximately 1/3 to 1/2 m from the axis. The predicted ion temperature agrees adequately with the charge-exchange temperature, bearing in mind the weak contribution made by thermal reactions to total neutron emission. It also agrees well with the crystal spectrometer temperature outside the beam heating interval. The line-averaged CXRS temperature is considered appropriate for comparison purposes because the central chords of the neutron profile monitor (based on line-integrated measurements) are given most weight in determining the core volume and elongation. The thermal neutron emission from the peripheral volume of the real plasma is assumed to be subsumed into the core, so the modelled ion temperature will tend to be higher than the line-averaged CXRS temperature.

Fig.6c compares the predicted electron temperature with the electron cyclotron emission (ECE) core volume-averaged values, with good agreement being achieved during the period of strong beam heating. Sawteeth were modelled empirically.

In summary, the discharge displays a strong Dα signal but no giant ELMs until well into the collapse phase. It exhibits a dominant beam-plasma component of neutron emission and the

beam-beam component is much larger than the thermal component. As mentioned earlier, this discharge was chosen because of its unexpectedly poor performance. In the event, the model simulates the discharge surprisingly well - which demonstrates that the assumed influx of cold neutrals can indeed simulate the slower inwards diffusion of gas fuelled ions and electrons to first order, so that for higher quality discharges with weaker recycling the simulations should be even better.

5.2 Discharge # 26087

The geometry for this discharge was similar to that for 25432, except that the X-point was formed on the upper, carbon, dump plates. The beam energy was partitioned to give 11 MW at 140 keV and 4 MW at 80 keV, with a 2-second period of beam pre-heating. Gas puffing during the main heating period was also used but was weaker than for 25432 and the discharge evolved into the highest performance discharge prior to the installation of the pumped divertor. This improvement is reflected in the core volume which, at 15 m^3, is almost double that for discharge 25432. The high performance phase terminated with a sawtooth crash and a giant ELM, followed by a carbon bloom.

For this discharge, the electron density profile was unusually strongly peaked, with the core-averaged density being 1.5 times the volume-averaged density. To accommodate this core density, the peripheral plasma volume was reduced in such a manner as to provide an entirely flat density profile while conserving the total number of particles. With this adjustment, the code models the total neutron emission rather precisely, as shown in fig. 7. The TRANSP calculation (not shown) gives very similar results. The beam-beam contribution is small compared with the thermal emission.

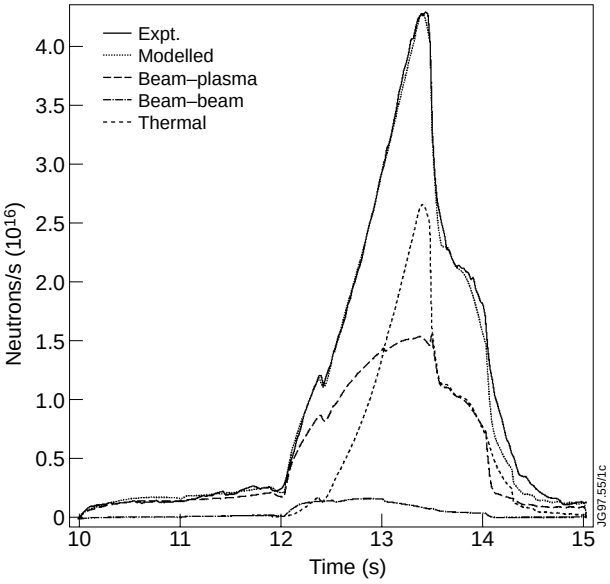

Fig.7: Showing the predicted neutron yields for the three neutron components for discharge 26087 . The dotted line represents the experimental total neutron yield. The results from the TRANSP simulation are similar. Note that the beam-beam contribution is now very small while the thermal contribution is dominant.

Figs.8a, b and c compare the predicted angular rotation rate, ion and electron temperatures with their experimentally determined counterparts. The calculated rotation rate is appreciably higher than the core-volume-average over the CXRS measurement. At least in part, this is attributed to the erratic behaviour of the measured rotation rate profile near the plasma axis, where the data indicate the existence of an on-axis minimum; extrapolation of the off-axis values towards the axis indicate that the true axial rotation rate is more in line

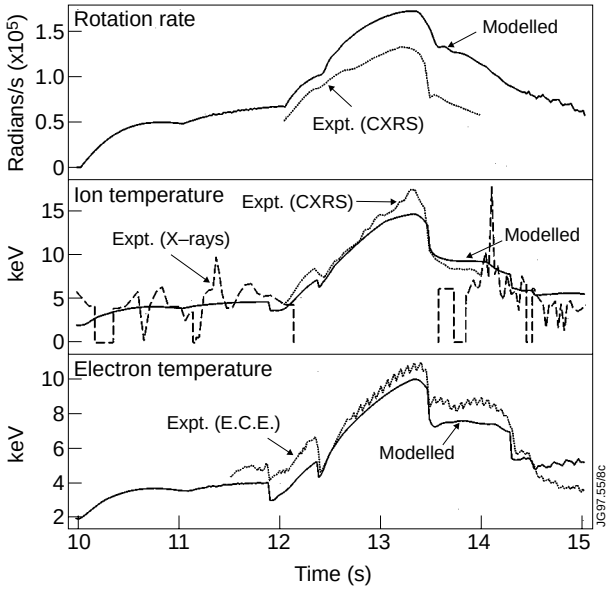

Fig.8: Comparing the predicted core rotation rate, ion and electron temperatures with available experimental data for discharge 26087. The CXRS ion temperature data are only obtainable during beam heating whereas the X-ray crystal data were only available when there was no beam heating.

with the predicted values. It is not necessary for the model to reproduce the measured rotation rate precisely, since the full effect of plasma rotation is to reduce the expected peak neutron emission strength by only 30%. The calculated ion temperature is in very good agreement with the line-averaged CXRS temperature. The measured electron temperature profile is relatively flat and fig. 8c shows acceptable agreement between prediction and measurement, although a little low after the neutron collapse.

We conclude that for this high performance discharge, the modelling of the gas puffing with cold neutrals proves generally satisfactory. However, this discharge has such strongly peaked temperature and density profiles that it is remarkable that the code performs as well as it does.

5.3 Discharge # 33643.

This is the first of three discharges studied for which the tokamak geometry was that of the Mk. I divertor, with the divertor coils being installed at the bottom of the vacuum vessel, so that the plasma axis was raised about 30 cm above the machine midplane and the beam ions were appreciably defocused. This defocusing naturally resulted in flatter ion temperature profiles, more appropriate than before for the application of the predictive model. The plasma volume was reduced from just over 100 m^3 to only 80 m^3. As determined by the neutron emission profile monitor, the core volume was 11 m^3, rather smaller than for discharge 26087. A mixture of 80 and 140 keV beam energies was employed in a strategy designed to optimize fuelling and heating so as to achieve higher neutron yields.

Fig.9 presents the measured total neutron emission with the calculated values obtained with the predictive model. The beam-plasma and beam-beam emissions are shown also. The neutron emission collapsed just before the beam heating was turned off because of the sawtooth crash and the near-simultaneous giant ELM. The quality of the fit of the predicted neutron emission profile to the measured profile at the moment of peak neutron yield is shown in fig. 10. The heights of the central channels of both cameras are reproduced accurately, which is an imposed requirement. Despite the use of top-hat profiles to represent the actual profiles and the use of pencil beams for computing the line-integrated yields, the overall fit is very good. The TRANSP

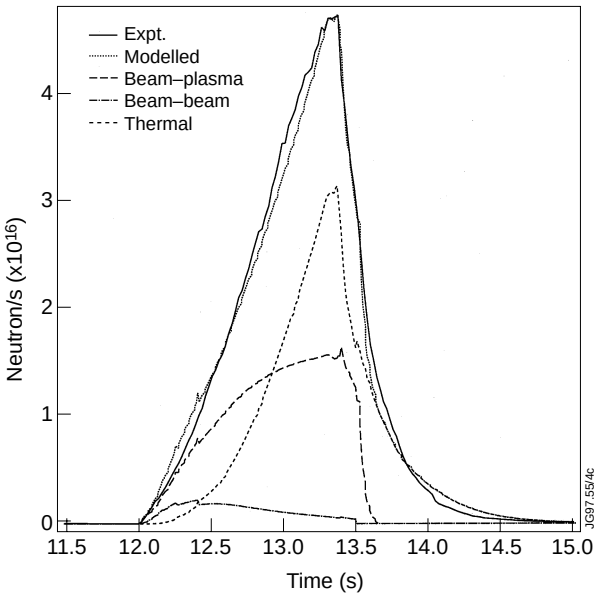

Fig.9: Showing the predicted neutron yields for the three neutron components for discharge 33643 . The dotted line represents the experimental total neutron yield. The results from the TRANSP simulation are similar.

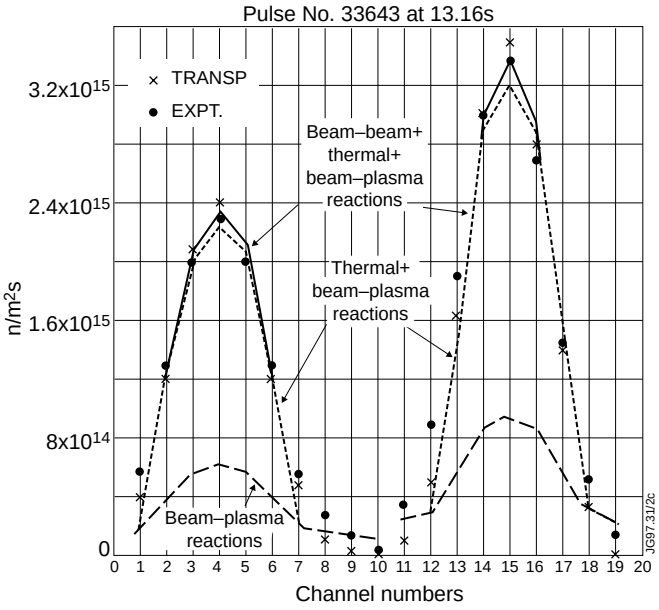

Fig.10: Comparing the predicted neutron emission profiles (lines) from thermal, beam-plasma and beam-beam reactions with experimental data (filled circles) recorded near peak performance for discharge 33643. The results of TRANSP simulations are also shown as crosses. The heights of the central channels of the two cameras are reproduced acceptably, which is an imposed requirement.

prediction also fits the experimental profile very closely. The profiles for discharges 33643, 34236 and 34500 are shifted vertically with respect to those for 25432 and 26087, corresponding to the different divertor configurations.

The model reproduces the volume averaged peak rotation rate obtained from the charge-exchange measurements rather well (fig. 11a) and also the general trend recorded with the crystal spectrometer data for the whole discharge, even though this is a local off-axis measurement. The ion temperature predictions (fig. 11b) agree closely with the line-averaged CXRS data during the beam heating period. Crystal spectrometer temperature data are available for the whole discharge, but are considerably lower as expected. The predicted

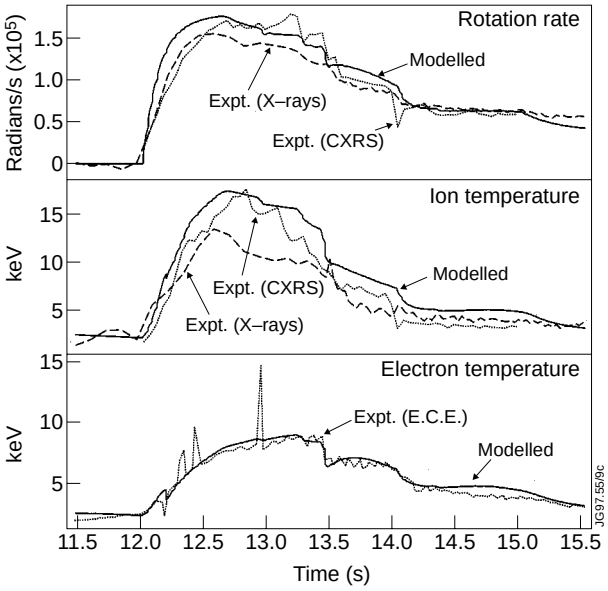

Fig.11: Comparing the predicted core rotation rate, ion and electron temperatures with available experimental data for discharge 33643. The charge-exchange data are only obtainable during beam heating.

electron temperature data agree very well with the volume-averaged temperature data provided by the ECE measurements (fig. 11c).

Overall, excellent agreement is found between the model predictions and all the experimental quantities for this high performance JET d-d discharge The modelling of the triton burnup signal will be considered in section 7.

5.4 Discharge # 34236

This discharge is one of the step-down series, comparable with 33643 except that the 80 keV beam power was reduced abruptly from 11 to 3 MW in an attempt to inhibit the first giant ELM. The idea was that the good confinement exhibited during the period when the neutron yield rose steadily might be retained with lower beam power, hence giving an increased energy confinement time [11].

Fig.12 compares the experimental total neutron emission rate with the results obtained with NEPAM. The overall agreement is very good. However, to model the slowly falling emission rate after the step-down (at 13 s), it was necessary to include a term representing ion and electron conduction losses. The Zeff, rotation rate and the Dα signal conspired to forbid the use of a large influx of neutrals to damp down the neutron yield after the step-down. The need for conduction losses suggests that the removal of the 80 keV beam heating of the peripheral volume has reduced the effective insulation offered to the core, with the result that conductive losses become noticeable.

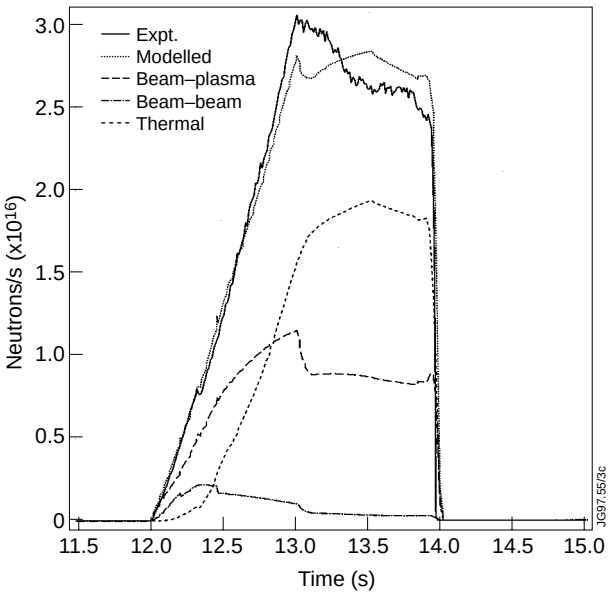

Fig.12: Showing the predicted neutron yields for the three neutron components for discharge 34236 . The dotted line represents the experimental total neutron yield. The results from the TRANSP simulation are similar..

The volume-averaged rotation rate provided by the charge-exchange measurements is compared with the model predictions in fig.13a. The instantaneous momentum transfer initially causes the plasma to accelerate faster than experimentally determined but the peak rotation rate is nevertheless only just achieved. The ion temperature measurements are compared with the calculations in fig.13b. The line-averaged CXRS ion temperature agrees well with the predicted temperatures. The X-ray crystal ion temperature falls below that of the CXRS measurement, as expected. The ECE volume-averaged electron temperatures are compared with the predictions in fig.13c. The predictions lie close to the measured data.

The analysis indicates that the energy confinement time rises steadily prior to the step-down and remains constant thereafter until the disruption. From a study of step-down discharges,

it is found that the behaviour of the neutron emission after the step-down is somewhat erratic, with large ELMs sometimes intervening and sometimes not. However, to produce discharges that can hold the neutron emission approximately constant at 3×10^{16} n.s^{-1} for over a second is a useful achievement.

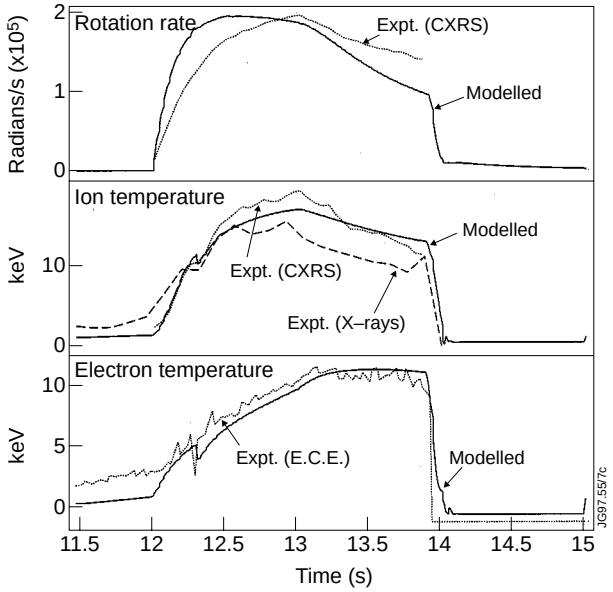

Fig.13: Comparing the predicted core rotation rate, ion and electron temperatures with available experimental data for discharge 34236.

5.5 Discharge # 34500.

The final example is a "failed" hot-ion H-mode discharge, characterized by a succession of giant ELMs commencing before the step-down in applied power. None of the ELMs was strong enough to terminate the discharge as with 26087 and 33643. This discharge is therefore an excellent subject for testing the modelling of the influx of cold neutrals.

The neutron emission predicted with the model is compared with the experimental values in fig.14. A reasonably good fit has been achieved, showing the near equality of the contributions from thermal and beam-plasma fusion reactions. The computed rotation rate, ion and electron temperatures (figs.15a-c) are all in acceptable agreement with their experimental counterparts.

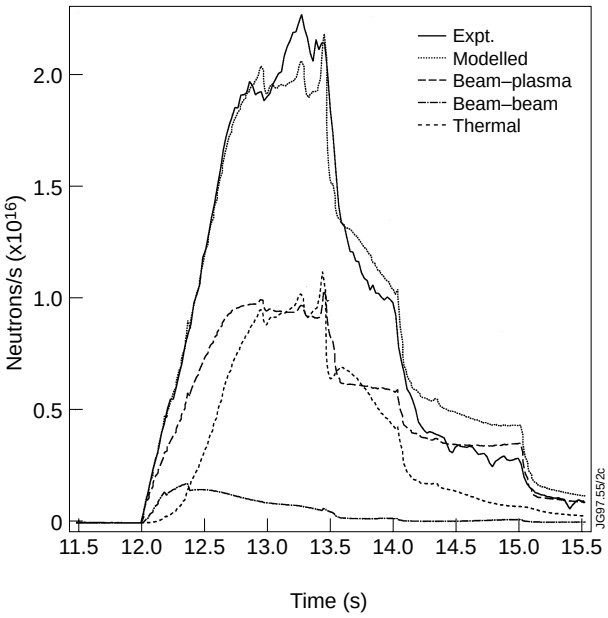

Fig.14: Showing the predicted neutron yields for the three neutron components for discharge 34500. The dotted line represents the experimental total neutron yield. The results from the TRANSP simulation are similar.

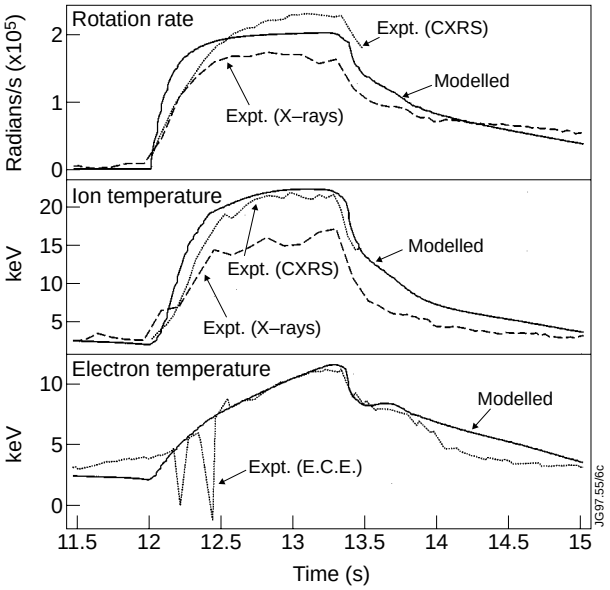

Fig.15: Comparing the predicted core rotation rate, ion and electron temperatures with available experimental data for discharge 34500.

6. BEAM-PLASMA AND BEAM-BEAM NEUTRON EMISSION

The three d-d neutron signals (thermal, beam-plasma and beam-beam) computed with TRANSP are sufficiently similar to those derived from NEPAM (figs. 5, 7, 9, 12 and 14) that they have not been displayed separately. The quality of the fits to the total neutron emission reflect the effort devoted to the relevant analyses. The beam-plasma emission calculations are compared in fig.16, where it can be seen that very close agreement is achieved. This agreement is only obtained when the beam ions are assumed to isotropize rapidly due to pitch-angle scattering. The tendency of the TRANSP calculation to be occasionally high is to be expected in so far as TRANSP also tends to over-estimate slightly the total neutron emission.

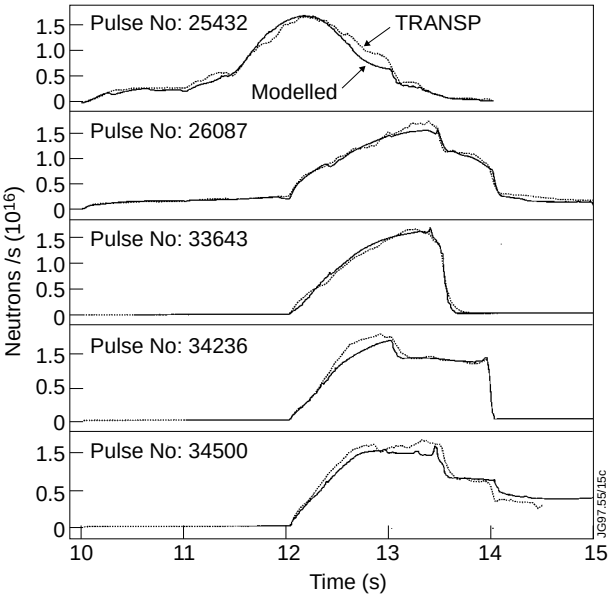

Fig.16: The predicted beam-plasma neutron production for the 5 discharges compared with the results of TRANSP simulations. The agreement is excellent.

The ability to calculate the beam-plasma neutron emission without requiring an exhaustive TRANSP analysis is of potential value in that the results can be used directly in the analysis of neutron energy spectra for high temperature discharges with thermal neutron emissivities comparable to or greater than the beam-thermal emissivity, a hitherto difficult domain for study. The beam-plasma neutron energy spectra can be computed using a Monte-Carlo approach [22].

Once the emission intensities associated with the different incident beam energy components have been calculated, then the neutron spectrum corresponding to thermal neutrons can be deduced and the axial ion temperature determined. The consistency of the measurements and calculations can then be tested.

The beam-beam neutron emission calculated with NEPAM is compared with the TRANSP results in fig.17. TRANSP has been used to determine the core volume reduction factors needed to estimate the square of the fast ion density (5 for the well-focussed beams using with the Mk.0 divertor and 2.5 subsequently), so the absolute magnitudes of the NEPAM predictions are effectively normalized to the TRANSP results. The time-dependencies agree very closely. Under normal conditions, the beam-beam contribution can be neglected.

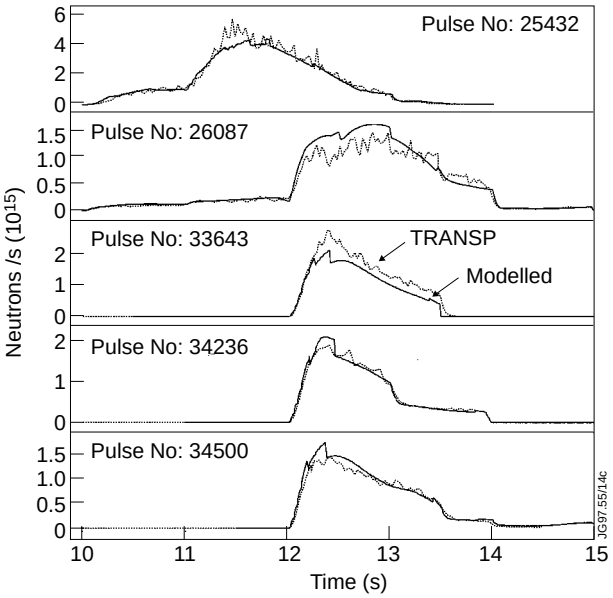

Fig.17: The predicted beam-beam neutron production for the 5 discharges compared with the results of TRANSP simulations. The agreement is clearly very good, due in part to the use of TRANSP to fix the absolute magnitude of the predicted signals.

7. THE TRITON BURNUP SIGNALS

The experimentally determined triton burnup signals are compared with the predictions form the code NEPAM and those from TRANSP analyses in fig.18. The solid lines present the experimental data, which should be assigned overall normalization uncertainties of about 10 to 20%. The dotted curves are the NEPAM predictions. In order to reproduce the experimentally observed time spread of the burnup signal, it was necessary to divide the triton population into two equal portions, one being localized in the core where they experience the full electron temperature, the other being restricted to the peripheral volume where they experience a lower effective

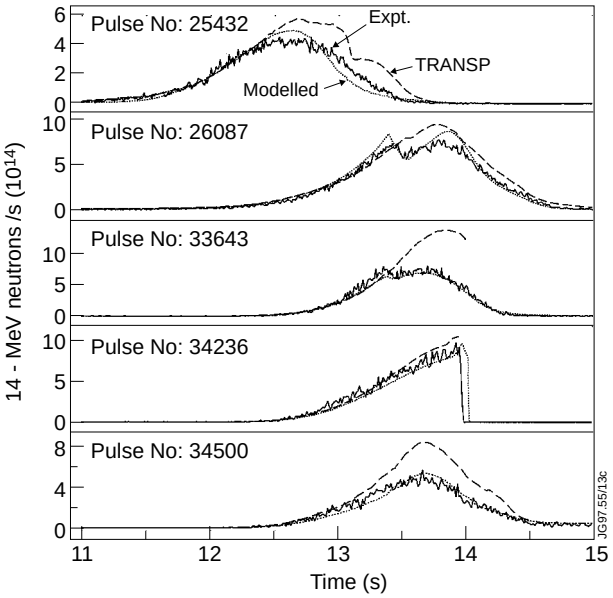

Fig.18: The measured 14 MeV neutron yields from triton burnup for the 5 discharges arecompared with predictions from the model and with the results from TRANSP simulations. The significant difference between the TRANSP and NEPAM calculations is manner in which charge-exchange losses are included in NEPAM (see text for explanation).

electron temperature (half the core temperature). The dashed lines are the TRANSP predictions, which should be more accurate since all the usual physical phenomena, neglected in the idealized NEPAM modelling, are fully represented.

The main difference between the NEPAM and TRANSP arises from the crude attempt with NEPAM to model charge exchange losses associated with the high neutral densities, especially during giant ELMs. It is suggested here that the neutral influx accompanying the giant ELM gives rise to a significant loss of tritons from the peripheral volume due to neutralization. For purposes of illustration, the core volume (passing) triton population is assumed to be little affected whereas the peripheral volume (including trapped) particles, encounter a neutral density set at a small multiple of the core neutral density. TRANSP also calculates charge-exchange losses, but the neutral densities are derived from questionable modelling of edge conditions and may not be correct.

Discharge 25432 has a very small core volume, as noted earlier, so charge-exchange losses of tritons are expected to be small due to significant re-ionization. No allowance has been made for neutralization losses of the tritons. The burnup fraction agrees almost precisely with the measurement, although the signal peaks a little early. The TRANSP over-prediction is mainly a result of over-estimating the d-d neutron emission during the collapse phase of the discharge.

The triton burnup signal for discharge 26087 is of particular interest. As shown more clearly in fig.19, the experimental data display a sudden dip at the time of occurrence of the giant ELM and nearly coincident sawtooth crash. The possibility that the dip might be of instrumental origin, related to pulse pile-up at the highest count rates, can be discounted by the observation that almost identical 14 MeV global emission time traces are provided by two distinct diagnostics - a silicon diode placed near a vacuum vessel diagnostic port [12] (from which the signal shown is derived) and the neutron emission profile monitor [14]. Except during the giant ELM, it is assumed that the recycling fuels the plasma by diffusion, and the neutral density is a fictional means for approximating the diffusive process. During the first giant ELM only, the computed neutral density is used as a source of triton charge-exchange losses from the plasma periphery.

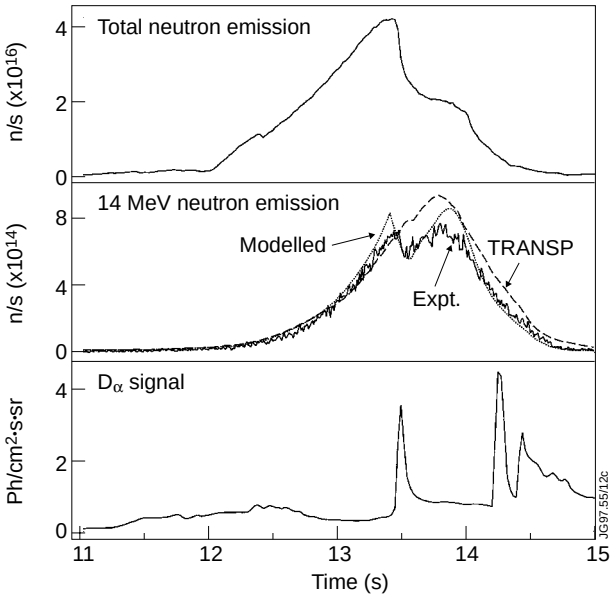

Fig.19: Showing the global 14 MeV neutron yield from triton burnup for discharge 26087 in relation to the d-d neutron yield and the Dα light signal. The predicted burnup yields from NEPAM and TRANSP are also shown. The dip at 13.5 s is attributed to losses of tritons due to charge-exchange events on neutrals brought in by the giant ELM, in coincidence with a sawtooth crash.

After the ELM, the low energy part of the triton distribution is refilled as the higher energy tritons slow down. As seen in fig. 19, an exaggerated dip in the global signal is produced. The TRANSP calculation over-estimates the burnup yield, as shown. Unexpectedly, the second giant ELM, at 14.2 s, does not produce a dip in the measured triton burnup signal although the spatial distribution of the slowing down tritons has not altered significantly. Relative to conditions at 13.5 s, the second ELM takes place in a plasma for which marked changes have occurred: the d-d neutron emission has fallen an order of magnitude, implying a much colder plasma, and the average electron density has increased 50%. Consequently, the penetration of charge-exchange neutrals into the plasma should much weaker. In addition, it may be pertinent that there is no coincident sawtooth crash.

Discharge 33643 also displays a definite dip in the experimental data coincident with the giant ELM. As usual, the triton burnup signal was modelled by dividing the triton population into two groups with different effective temperatures so as to enforce agreement between the shapes of the calculated and experimental time-dependent signals prior to the plasma collapse; however, in this case, the triton neutralization losses were assumed to occur throughout the discharge, not just during the ELM, so the drop due to the ELM is less than that observed. Omitting the neutralization losses altogether results in a gross over-estimate of the burnup signal, closely similar to that exhibited by the TRANSP calculation.

The triton burnup signals computed with NEPAM and with TRANSP for discharge 34236 both display good agreement with the measured data up to the major disruption at 13.9 s. This quality of agreement is expected because of the low level of neutral influx prior to the collapse.

Finally, an excellent fit to the data has been achieved for discharge 34500 using the customary neutral density as a source of neutralization losses. Without such losses, the burnup signal would have been doubled, to agree with the TRANSP prediction.

From these examples, it is seen that TRANSP fails to provide acceptable fits to the triton burnup measurements for these hot-ion H-mode discharges, although some improvement could doubtless be achieved if a more faithful modelling of the discharge terminations were to be attempted. Even so, it is doubtful that the dips observed in discharges 26087 and 33643 could be easily reproduced. The triton neutralization losses modelled in NEPAM are evidently able to reproduce the observed effects, which indicates a possible explanation for the discrepancy. It should be noted that giant ELMs only rarely produce sudden dips in the triton burnup signal. It seems likely that a near coincidence between a giant ELM and a sawtooth crash is a necessary condition for their occurrence. Sawteeth affect the orbits of fast particles in the plasma, and the there is evidence [23] that particles on passing orbits near the plasma centre are most affected, being transferred to trapped orbits with large banana widths which therefore explore the outer reaches of the plasma where the neutral density would be greatest.

8. CONCLUSIONS

The simple model presented here is capable of predicting the instantaneous neutron emission strength from low recycling, hot-ion H-mode discharges with surprising accuracy up to the moment that MHD-related events intervene. By using the Dα recycling signal to simulate edge fuelling of the plasma (implemented as an influx of neutral fuel atoms distributed uniformly over the plasma volume), it is found that the neutron emission from the entire discharge, including the termination, can be modelled even when the recycling is strong. That this results in reasonable values of core ion and electron temperatures, simulates the plasma rotation rate rather well, and provides an explanation for the anomalous behaviour of the triton burnup signal, indicates that a deep incursion of neutral atoms into the peripheral volume is very likely during giant ELMs but should not be taken to indicate that the neutral cascade is reaching into the core. Turbulent mixing processes as well as sawtooth crashes probably play a major role in the plasma interior. That there exists a linear relationship between the toroidal momentum slowing down times and the energy confinement times has been demonstrated by Zastrow et al [24]; a relationship of this sort is expected as a natural consequence of the present model.

Since the model is successful in reproducing the neutron emission from typical high performance JET discharges, it can be used with some confidence for investigating the effects of altering the discharge conditions (e.g. starting densities, Zeff, heating powers and beam energies). Furthermore, by using the ITERH93-P scaling law for confinement time as a definition of the energy loss rate, the first order effects of changing the plasma geometrical parameters can also be studied. Finally, starting from an optimized d-d plasma discharge, the analogous d-t discharge, including alpha-particle heating effects, can be modelled with some confidence since the transport coefficients for deuterium and tritium are known to be very similar so that the fusion yields will differ mainly through their respective atomic and nuclear cross-sections.

ACKNOWLEDGEMENTS

The author is grateful to Dr. W.Core for assistance with the implementation of the reaction rate formulae and to Dr. F.B.Marcus for numerous suggestions made during the course of the work.

REFERENCES

[1] R.V.Budny et al., Nuclear Fusion **32** (1992) 429.

[2] O.N.Jarvis, J.M.Adams, F.B.Marcus and G.Sadler, "Neutron Profile Measurements in JET", JET-P(95)67. 7th Int. Conf. on Plasma Physics and Controlled Nuclear Fusion, Toki-City, Japan, 1995. To be published in Fusion Engineering and Design.

[3] F.B.Marcus et al., Rev. Sci. Instrum. 68(1), January 1997.

[4] K.Thomsen, D.J.Campbell. J.G.Cordey, et al., Nuclear Fusion **34** (1994) 131.

[5] J. Wesson and B. Balet, "Abrupt changes in confinement in the JET tokamak", JET-P(96)19.

[6] J.P.Christiansen and D.Muir, " Rapid changes to confinement and/or heating", EU-US Workshop on Transport in Fusion Plasmas, Varenna, 2-5 September, 1996. To appear as JET-P(96)38.

[7] F.B.Marcus et al., "A power step-down approach to high performance, steady-state operation with ELM-free H-mode deuterium plasmas at JET", JET-P(96)59. To be published in Nuclear Fusion.

[8] L.C.Johnson and E.Hinnov, J.Quant. Spec. & Rad. Trans. **13** (9173) 333.

[9] W.G.F. Core, P. van Belle and G.Sadler, "Beam-plasma fusion yields in Rotating Tokamak Plasmas". 14th European Conference on Controlled Fusion and Plasma Physics, Madrid, 22-26 June 1987.

[10] T.Elevant, P. van Belle, O.N.Jarvis, G.Sadler, Nucl. Instrum. and Meth. in Phys. Res. **A364** (1995) 333-341.

[11] F.B.Marcus, J.M.Adams, D.S.Bond et al., Nuclear Fusion **34** (1994) 687.

[12] S.Conroy, O.N.Jarvis, M.Pillon and G.Sadler, "A regime showing anomalous triton burnup in JET", Controlled Fusion and Plasma Heating (Proc. 17th Europ. Conf. Amsterdam, 1990), Vol **14B**, Part I, European Physical Society (1990), p.98 .

[13] J.D.Strachan, J.Scott McCauley, T.Munsat et al., Nuclear Fusion 36 (1996) 1189

[14] O.N.Jarvis, J.M.Adams, S.W.Conroy et al., "Triton burnup in JET - Profile effects", Controlled Fusion and Plasma Physics (Proc. 18th Europ. Conf. Berlin, 1991), Vol 15C, Part I, European Physical Society (1991), p.21

[15] The JET Team (presented by P.R.Thomas), in Plasma Physics and Controlled Fusion Research 1996 (Proc. 16th Int. Conf. Montreal, 1996), IAEA Vienna (1996), Paper IAEA-CN-64/A3-2.

[16] J.Wesson, "Tokamaks", Clarendon Press, Oxford, 1987.

[17] T.Stix, Plasma Phys. **14** (1972)367.

[18] W.G.F.Core and K-D Zastrow, JET-R(96)01.

[19] The JET Team, Nucl. Fusion **32**(1992)187.

[20] M. von Hellermann et al., "Feasibility of quantitative spectroscopy on ITER", JET-P(95)63 and in Diagnostics for Experimental Thermonuclear Reactors, Plenum Press, New York and London (1966), pp. 385-395.

[21] R.Bartiromo, F.Bombarda, R.Giannella et al., Rev. Sci. Instrum. **60** (1989) 237.

[22] P. van Belle and G.J.Sadler, "The computation of fusion product spectra from high temperature plasmas", in Basic and Advanced Diagnostic Techniques for Fusion Plasmas, Varenna 1986. CEC Brussels, EUR 10797 EN, Vol. III (1987).

[23] O.N.Jarvis, J.M.Adams, P.J.A.Howarth et al., Nuclear Fusion **36** (1996) 1513.

[24] K-D. Zastrow, J.C.M de Haas, M.G. von Hellermann et al, "Toroidal momentum slowing down and replacement times in JET divertor discharges", Controlled Fusion and Plasma Physics, (Proc. 22nd Europ. Phys. Soc. Conf, Bournemouth, 1995)Vol. 19C, Part II, pp. 453-456.